Influence of Molecular Weight Distribution on Flow Properties of Commercial Polyolefins

Mostafa Zahedi,[1] Mostafa Ahmadi,[2] Mehdi Nekoomanesh[2]

[1]*JAM Petrochemical Co., R&D Center, Bandar Asalooyeh, Asalooyeh, Iran*
[2]*Department of Polymerization Engineering, Iran Polymer and Petrochemical Institute, Tehran, I.R. Iran*

Received 12 September 2007; accepted 29 December 2007
DOI 10.1002/app.28035
Published online 6 March 2008 in Wiley InterScience (www.interscience.wiley.com).

ABSTRACT: The aim of this work is to investigate the effects of molecular weight distribution on some conventional flow properties of polyolefins like melt flow index, melt flow ratio, and power law index. The study is designed in two steps. First, the statistical correlation analysis was carried out for proper choice of input variables for each output property and to find the most relevant mathematical forms of the considered parameters for the modeling section. Then the considered property was correlated to the entire molecular weight distribution using spline functions. The best fit was achieved by variation of the number of spline nodes and their values. The proposed methodology is able to be coupled with a polymerization model to correlate the polymerization conditions to the final properties of the product and design a polymerization control loop. © 2008 Wiley Periodicals, Inc. J Appl Polym Sci 108: 3565–3571, 2008

Key words: melt flow index; melt flow ratio; power law index; molecular weight distribution; structure property relationship

INTRODUCTION

Various aspects of chain microstructure such as molecular weight (MW) and its distribution (MWD), comonomer content and its distribution, long chain branching (LCB) and its distribution are essential characteristics which determine the final properties of polymers. Quantification of structure properties relationship (SPR) has been an enduring issue in polymer science. Such knowledge helps to design the necessary microstructure for a series of desired properties by controlling polymerization conditions.[1]

Melt flow index (MFI) is a well-known conventional index of processability and product quality. The data obtained by this method should be interpreted carefully, because this method suffers from several shortcomings.[2] First, the results cannot be accepted as a good indicator of processability because of the differences that exist in the applied shear rates of the MFI test and various processing methods and, in addition, shear dependence of polymers viscosities. Second, reproducibility of the results is very sensitive to details of the measurement procedure. But having all of these shortcomings, MFI is deeply embedded in plastic technologies as a practical criterion of product quality. Therefore, it is really beneficial to establish a quantitative relationship between MFI and microstructural parameters like MWD. This information helps polymerization engineers to provide relationships between polymerization conditions and the final properties as well.

Mechanical properties are mainly dependent to MW, whereas MWD is responsible for rheological properties. Entanglements of long polymer chains make their behavior different from elastic solids and viscose liquids.[3] Entanglements appear after increase of the chain length above a critical value, which is believed to be about double of the length between two subsequent entanglements (M_e).[4] Occurrence of entanglements above this critical length leads to dependence of zero shear rate viscosity to a certain power of MW about 3.2–3.6, whereas this relationship is proportional below the critical length.

Pouiselle's equation (flow rate of Newtonian liquids in a capillary) gives the relationship between MFI and Newtonian viscosity of polymers in low shear rate regions as follows:

$$\mathrm{MFI} = 600\rho\, Q \text{ and } Q = \frac{\pi R^4 \Delta P}{8\eta L} \tag{1}$$

The relationship between MFI and MW can be derived using the dependence of zero shear rate viscosity to the MW as follows:

$$\eta_0 = kM^{\alpha} \Rightarrow \mathrm{MFI} = k'M^{-\alpha} \tag{2}$$

It should be noted that only the MFI results by the load of 2.16 kg are applicable in eq. (2), because polymer viscosity is in the non-Newtonian regions at

Correspondence to: M. Ahmadi (m.ahmadi@ippi.ac.ir).

Journal of Applied Polymer Science, Vol. 108, 3565–3571 (2008)

TABLE I
GPC and MFI Results of Commercial Polyolefin Samples

		GPC results			MFI results				
Sample	Type	M_n	M_w	PDI	2.16 kg	5 kg	10 kg	15 kg	21.6 kg
A	HDPE	13,700	57,100	4.15	4.34	12.49	33.83	62.26	106.89
B	HDPE	19,700	58,200	2.96	4.01	11.28	30.31	53.67	99.54
C	HDPE	13,000	59,400	4.58	4.49	12.78	33.84	60.61	111.94
D	HDPE	9,500	40,100	4.23	17.51	48.61	127.23	225.50	389.77
E	HDPE	16,400	106,700	6.51	0.52	1.78	5.33	11.34	22.11
F	HDPE	6,500	143,200	22.21	0.10	0.44	1.73	4.45	10.77
G	HDPE	13,900	135,800	9.77	0.10	0.61	2.20	5.09	12.54
H	HDPE	5,900	157,400	26.64	0.07	0.33	1.34	3.35	8.58
I	HDPE	7,900	52,100	6.61	7.96	24.09	64.94	123.21	228.40
J	PP	32,200	114,000	3.54	16.88	64.88	270.75	380.21	381.17
K	PP	28,100	128,000	4.56	10.21	40.00	167.53	378.14	380.40
L	PP	54,000	204,000	3.77	2.16	8.55	35.73	95.78	275.82

higher loads. Many parameters make the MFI of commercial polymers to deviate from eq. (2).[5,6] Wooden et al.[7] have proposed the following equation in presence of oils, oligomers, and monomers in the sample:

$$\ln(\mathrm{MFI}) = 22.15 - 3.79\ln(M_w) + 0.255\ \mathrm{Oil} + 0.189\ \mathrm{Oligomer} + 0.495\ \mathrm{Monomer} \quad (3)$$

Todd et al.[8] have reported the following equation for considering the effect of broad MWD of bimodal polymers:

$$\mathrm{MFI} = 1.85E18\left(\frac{M_w}{\mathrm{PDI}^{0.202}}\right)^{-3.65} \quad (4)$$

However, Ariawan et al.[9] have noted that increase of polydispersity index (PDI) by adding a tail to high or low MW regions of MWD exerts opposite effects on MFI and, therefore, it is better to correlate the MFI to the entire MWD instead of PDI. Some authors have recently correlated the MFI to slices of MWD to determine the most critical portions of MWD in the formation of MFI.[9,10] Nele et al.[11] have correlated MFI to the exact weight fractions of different chains using cubic splines. Such an approach combined with a polymerization modeling can be directly used in developing a control loop which correlates the reactor's operational conditions to the end-use properties.

In this work, the quantitative dependence of several industrial flow properties on the MWD was found to better understand their molecular source and to develop practical means for correlating polymerization condition to the end-use properties in the subsequent works. First, the statistical correlation analysis between structural parameters and flow properties of MFI, melt flow ratio (MFR), and power law index has been carried out. Then this analysis has been used for proper choice of input parameters and mathematical form of the kernel function for modeling of structure dependence of each property.

EXPERIMENTAL

Nine commercial high-density polyethylene (HDPE) samples and three commercial polypropylene (PP) samples with various distributions of molecular weight were selected from different producers. Their MWDs were determined using gel permeation chromatography (GPC) (PL-210) at 140°C using 1,2,4-trichlorobenzene as solvent. Obtained molecular weight averages are listed in Table I. The MFI values with loads of 2.16, 5, 10, 15, and 21.6 kg were measured by means of a melt flow tester (CEAST) according to ASTM D 1238. The MFI of the HDPE and PP sample were measured at 190 and 230°C, respectively. Table I shows the MFI results of all samples as well.

Modeling

This section provides detailed information about correlating a scalar value to a spectrum. Figure 1 shows the essential elements of the modeling loop. These elements are the kernel function, the mixing rule, and the optimization algorithm, respectively. The kernel function calculates the objective property as a function of the considered structural parameters for a single isolated chain. Various mathematical functions can be used as the kernel function, including a simple polynomial of the degree of n or an empirical function. Although theoretically derived functions based on polymer dynamic theories can be applied for rheological properties,[4,12] it is more convenient to use simpler mathematical functions for practical purposes. Though reptation models can predict the behavior of a single chain accurately and their predictions cannot be compared by predictions of sim-

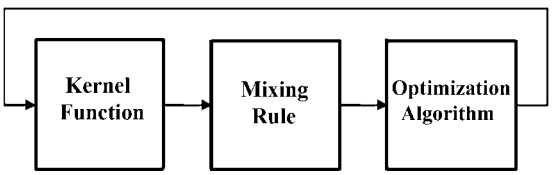

Figure 1 Essential elements of the modeling loop.

ple mathematical functions, the cumulative results are similar. In fact theoretical models are favorable for investigating the behavior of different chains, while simpler mathematical models like splines are more suitable for predicting the measured property neglecting the mechanism behind it. We used cubic splines with different numbers of nodes as the kernel function. One of the goals in this work is to find the optimum number of splines for the mentioned specific problem.

After calculation of the considered property for all the chains, a mixing rule is used for summation of the contribution of various chains and their mutual interactions. Flow of longer chains accelerates in the presence of shorter chains in a polydisperse system. Therefore nonlinear mixing rules are used in reptation models to consider these interactions.[13–16] In this model one can use a linear mixing rule, and these interactions will be appeared in the shape of spline curves as follows:

$$\log(\mathrm{MFI}) = \int_1^\infty f(M)w(M)d\log(M) \tag{5}$$

where the logarithmic form of the parameters was selected according to statistical analysis (Table II). Finally, the calculated property should be compared by the measured values and differences should be minimized by an optimization algorithm. The Nelder-Mead simplex method[16,17] was used as the multivariable nonlinear optimization algorithm which finds the optimal node values to minimize the *R*-squared parameter as follows:

$$R\text{-squared} = 1 - \left(\sum_{i=1}^{n}(V_{\mathrm{exp}} - V_{\mathrm{pre}})^2\right) \Bigg/ \left[\sum_{i=1}^{n} V_{\mathrm{exp}}^2 - \left(\sum_{i=1}^{n} V_{\mathrm{exp}}\right)^2 \Bigg/ n\right] \tag{6}$$

where V is the considered parameter like MFI and n is the number of experimental values. The Nelder-Mead simplex method finds a local minimum of a function of p variables. The search starts with points in a simplex consisting of $p + 1$ vertices, not all in the same plane, in a feasible region. It proceeds by continuously dropping the worst point in the simplex and adding a new point determined by the reflection of the worst point through the centric of the remaining vertices.

It is important to note that because the amounts of very short and very long chains are too low, the values of two boundary nodes at molecular weights of 10^2 and 10^8 were inevitably set to zero to prevent the divergence of the optimization algorithm.

RESULTS AND DISCUSSION

With the set of commercial polyolefins covering broad range of MWD, it was possible to study the effects of microstructure on the considered properties. At the first step, the statistical correlation analysis[18] was carried out between relevant forms of input parameters and output properties of HDPE samples. Table II shows the correlation factors for molecular weight averages and MFI. Two statistical correlation factors were used for evaluating the strength of correlations. Pearson product moment (PPM) varies between −1 and +1 and measures the strength of the linear relationship between each pair of variables. The most independent variables have zero PPM. The second statistical correlation factor is the statistical significance (*P*-value) of the estimated correlations. *P*-values below 0.05 indicate statistically significant correlations at the 95% confidence level.

Table II shows that the most correlated variables are the log(MFI) and log(M_w), where M_w is the weight average MW. Equation (7) presents the linear regression result and the corresponding *R*-squared value as a quantitative indicator of the prediction's quality.

$$\log(\mathrm{MFI}) = 20.41 - 4.15 \times \log(M_w), \quad R\text{-squared} = 99.25 \tag{7}$$

Figure 2(a) illustrates the quality of predictions. It is obvious that the equation provides a good description of the experimental data, but the error mainly comes from higher MFI values. This deviation is due to consideration of the logarithmic form of MFI which reduces the higher errors. Therefore the eq. (2) was used to correlate the MFI to a certain power of M_w. The k' and α were adjusted by Nelder-Mead optimization method, while the target function was *R*-squared from eq. (6). Equation (8) and Figure 2(b)

TABLE II
Statistical Correlation Analysis Between MFI and Molecular Weight Averages

Parameter	Factors	Log(M_w)	Log(M_n)	M_w	PDI
Log(MFI)	PPM	−0.996	0.327	−0.994	−0.807
	P-value	0	0.391	0	0.009
MFI	PPM	−0.8304	−0.0373	−0.7610	−0.5026
	P-value	0.0056	0.9241	0.0172	0.1679

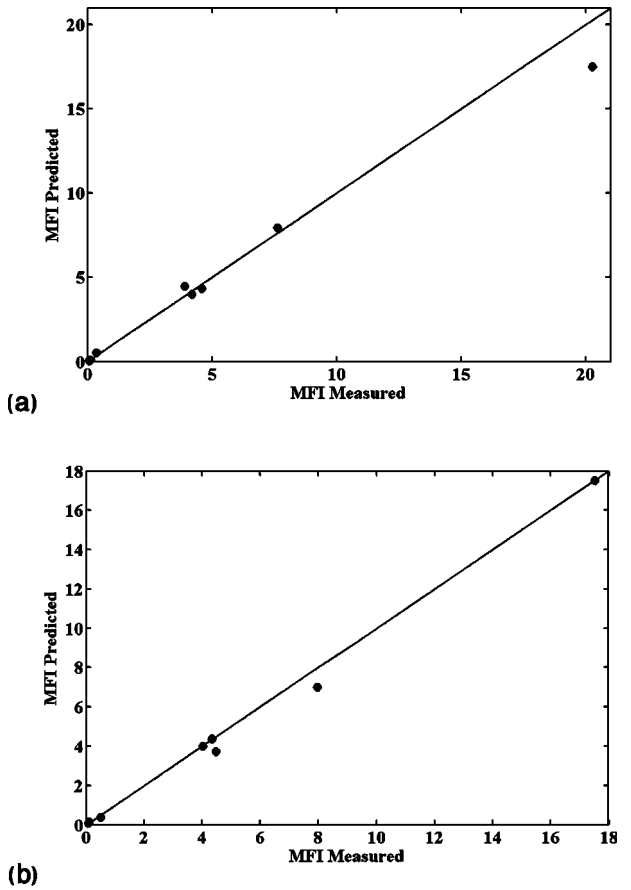

Figure 2 Measured MFI values of HDPE samples versus predictions of (a) the linear regression and (b) Nelder-Mead optimization method, using average MW values.

show how the predictions have improved.

$$\text{MFI} = (6.09 \times 10^{17}) \times M_w^{-3.59}, \qquad R\text{-squared} = 99.99 \tag{8}$$

Equation (3) was then used to correlate the same set of experimental data to the entire MWD. Different numbers of spline nodes were tried for achieving the best modeling results. Values of two boundary nodes were set to zero and the values of interior nodes were adjusted by optimization algorithm. Conditions of different modeling runs and their results are listed in Table III. Figure 3(a) shows the kernel function obtained by four nodes. The corresponding *R*-squared shows that the predictions are not so good. The slopes of the kernel function at two boundary nodes were also set to zero to achieve more realistic results. Figure 3(b) and the corresponding *R*-squared indicate that the correction has positive effect on the quality of predictions. Figures 4(a,b) show the curve obtained by five nodes and the predictions quality. The improvement is admittedly significant. Figure 5(a) shows the curve obtained by seven nodes. The corresponding *R*-squared shows that the improvement is not so significant while the amount of numerical calculations was considerably increased. Figure 5(b) shows the curve belonging to nine nodes. It is obvious that the flexible nature of the solution has leaded to an unrealistic result that is not interpretable. Thus the optimal number of nodes is equal to 5.

The optimal solution was also applied to MFI results obtained by loads of 10 and 21.6 kg. Figure 6 shows the kernel functions obtained by different loads. As a qualitative interpretation, it seems that the shorter chains tend to increase the MFI whereas the longer chains tend to decrease it. This observation was expected as it was explained in definition of the mutual interactions of different chains in the modeling section. In fact, longer chains have the most contribution in formation of entanglements whereas shorter chains tend to lower the entanglement density by creating gap between long chains. Therefore, the flow of longer chains speeds up in the presence of further shorter chains. Figure 6 also indicates that the positive contribution of shorter chains increases and the negative contribution of longer chain decreases as the applied load increases. This behavior implies that the entanglement density decreases by increase of applied shear rate, and therefore the role of longer chains diminishes whereas the role of shorter chains increases by faster relaxation.

TABLE III
Conditions of Different Modeling Runs and Their Results

Run	Samples	Parameter	Slope	Interior nodes: Log(*M*)	*R*-squared
1	HD	MFI 2.16 kg	−	[4 6]	82.41
2	HD	MFI 2.16 kg	+	[4 6]	93.99
3	HD	MFI 2.16 kg	+	[3 5 7]	99.40
4	HD	MFI 2.16 kg	+	[3 4 5 6 7]	99.55
5	HD	MFI 2.16 kg	+	[2.8 3.6 4.4 5.1 5.9 6.5 7.2]	99.63
6	HD	MFI 10 kg	+	[3 5 7]	99.57
7	HD	MFI 21.6 kg	+	[3 5 7]	99.49
8	PP	MFI 2.16 kg	+	[3 5 7]	99.44
9	HD	MFR4	+	[3 5 7]	96.02
10	HD	*n*	+	[3 5 7]	96.12

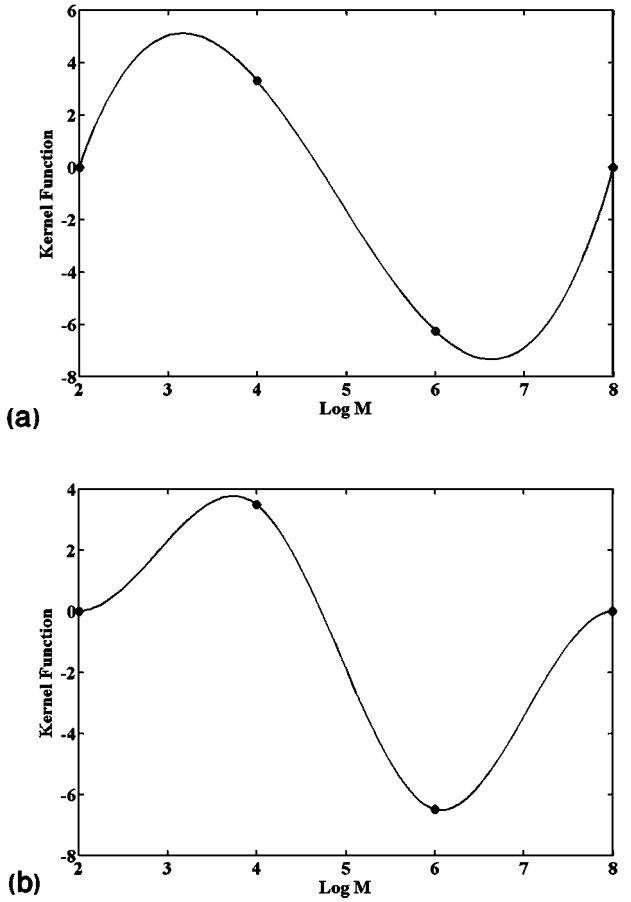

Figure 3 Kernel functions obtained by four nodes (a) without zero boundary slope and (b) with zero boundary slope.

Figure 7 compares the kernel function obtained for HDPE and PP samples. It is clear that the shape of the obtained curves are very similar, implying that the flow characteristics of linear chains only depends to entanglements which is a function of the chain length. The relative contribution of two types of polymers in Figure 7 can be attributed to relative flexibility of the chains. The presence of regular side methyl groups in PP chains provides more difficulties for coiling and therefore lowers entanglements in comparison with HDPE chains.

The MFR is usually used as an indicator of dispersity of the MW. Thus, the statistical correlation analysis was performed for these parameters as well. Table IV shows the correlation factors between more correlated MFRs and molecular weight averages. The highest correlation exists between PDI and MFR6. Equation (9) presents the corresponding linear relationship.

$$\mathrm{PDI} = -12.87 + 3.42 \times \mathrm{MFR6}, \quad R\text{-squared} = 88.77 \tag{9}$$

Table IV also shows that MFR4 is more dependent on the MW. Equation (10) shows this relationship as follows:

$$\mathrm{MFR4} = 1.50 + (3 \times 10^{-5}) \times M_w, \quad R\text{-squared} = 94.42 \tag{10}$$

The power law equation is the most common model in description of the non-Newtonian region of viscosity versus shear rate plot. The power law index (n) can be calculated using the following equation:

$$Q = \frac{n\pi R^3}{3n+1}\left(\frac{R\Delta P}{2kL}\right)^{1/n} \Rightarrow \log(MFI) = \mathrm{Constant} + \frac{1}{n}\log(\mathrm{Load}) \tag{11}$$

Table IV shows that the power law index significantly depends to the M_w and consequently to the MFR4. These relationships are presented in eqs. (12)

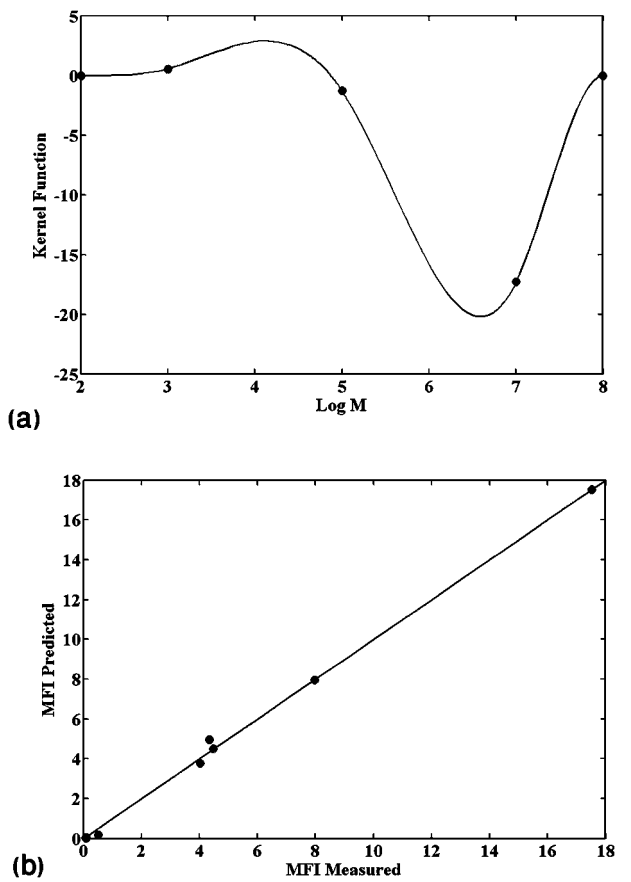

Figure 4 Results obtained by five nodes (a) the kernel function and (b) measured MFI values versus predicted ones.

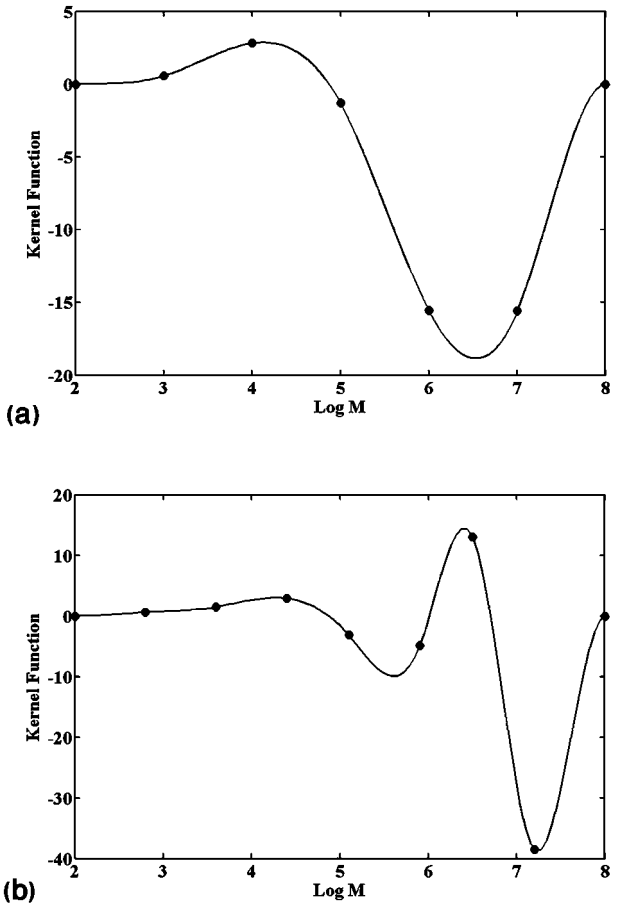

Figure 5 Kernel functions obtained by (a) seven spline nodes and (b) nine spline nodes.

and (13) as follows:

$$n = 0.86 - (2.45 \times 10^{-6}) \times M_w, \quad R\text{-squared} = 95.93 \tag{12}$$

$$n = 0.97 - (7.96 \times 10^{-2}) \times \text{MFR4}, \ R\text{-squared} = 97.17 \tag{13}$$

The MFR4 and power law index were correlated to the entire MWD using the following equation, according to the results of statistical correlation analysis:

$$\text{MFR} = \int_0^\infty f(M)w(M)dM \tag{14}$$

Modeling results are listed in Table III as well. Figure 8 shows the obtained kernel functions. Figure 8(a) implies that the MFR increases as the weight fraction of polymer chains in low or high molecular weight regions increases. This behavior was expected because PDI rises by increase of tails in low- or high-molecular weight regions and also it is proportional to the PDI. Figure 8(b) shows the kernel function obtained for the power law index. The obtained curve is similar to the previous curve, which was anticipated because of linear relationship between MFR4 and the power law index. The obtained curve implies that polymer shear thinning is proportional to the PDI as well.

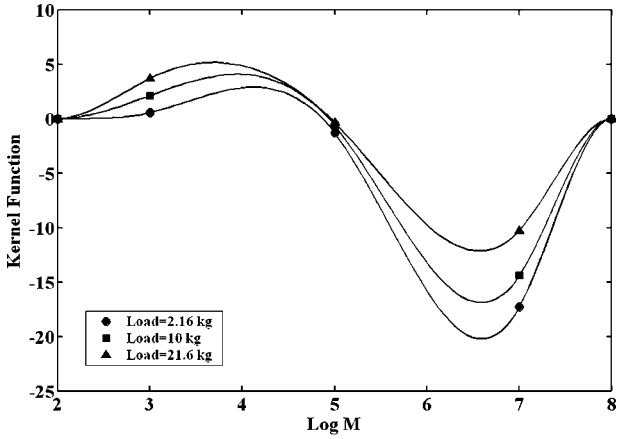

Figure 6 Kernel functions obtained for MFI values of HDPE samples at different loads.

CONCLUSIONS

A method for correlating polymer end-use properties to the entire MWD was presented. The optimal conditions of modeling variables were found to achieve the best results in the optimum amount of calculations. It was found that more precise predictions can be made by considering the effect of whole MWD instead of average values like M_w or PDI. But higher precision is not the main proceed. Use of splines provides a visual interpretation of the physics behind each property and can also be used in combination with a polymerization model for control pur-

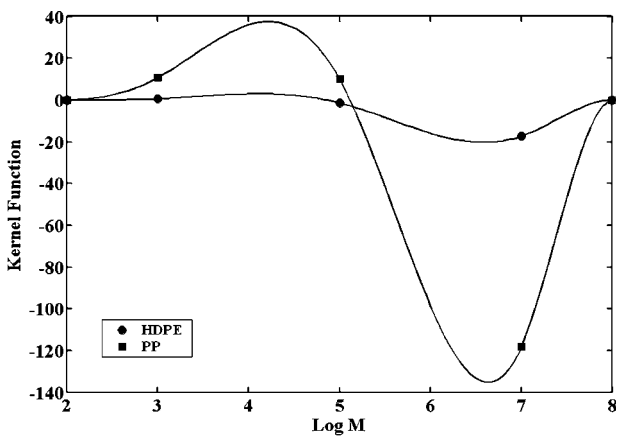

Figure 7 Kernel functions obtained for MFI values of HDPE and PP samples.

TABLE IV
Statistical Correlation Analysis Between MFR, Power Law Index, and M_w

Parameter	Factors	MFR4 (10/5)	MFR5 (21.6/10)	MFR6 (15/5)	MFR7 (10/2.16)	MFR8 (21.6/5)	n
M_w	PPM	0.975	0.857	0.965	0.928	0.963	−0.981
	P-value	0	0.003	0	0	0	0
Log M_w	PPM	0.945	0.840	0.932	0.901	0.928	−0.964
	P-value	0	0.005	0	0.001	0	0
PDI	PPM	0.912	0.612	0.942	0.765	0.938	−0.840
	P-value	0.001	0.080	0	0.016	0	0.005

poses. It was shown that the long chains tend to lower the MFI by increasing the entanglements, whereas the short chains tend to increase it by fast relaxation. It was also indicated that the negative influence of longer chains was decreased and the positive influence of shorter chains was increased as the entanglements were lowered by increase of the applied load. The linear relationship between MFR, PDI, and the power law index were revealed which leads to similar dependences of MFR and power law index to the MWD. It was shown that these parameters enhance as the weight fractions of shorter and longer chains increase.

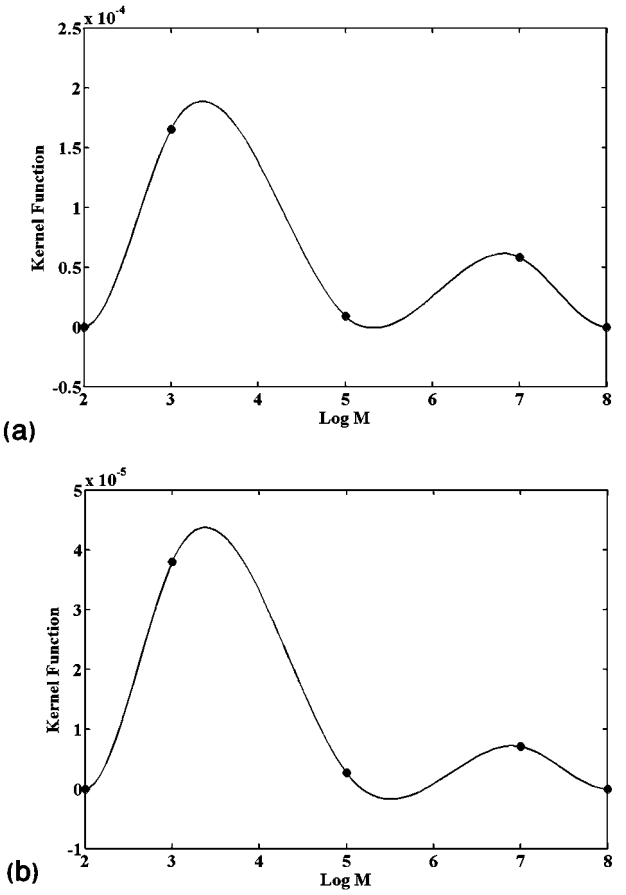

Figure 8 Kernel functions obtained for (a) MFR4 and (b) power law index of HDPE samples.

References

1. Valappil, J.; Georgakis, C. AIChE J 2002, 48, 2006.
2. Bremner, T.; Rudin, A. J Appl Polym Sci 1990, 41, 1617.
3. Ferry, J. D.; Viscoelastic Properties of Polymers; Wiley: New York, 1980.
4. Doi, M.; Edwards, S. F. The Theory of Polymer Dynamics; Clarendon Press: Oxford, 1986.
5. Latado, A.; Embiruc, M.; Mattos Neto, A. G.; Pinto, J. C. Polym Test 2001, 20, 419.
6. Teresa Rodriguez-Hernandez, M.; Angulo-Sanchez, J. L.; Perez-Chantaco, A. J Appl Polym Sci 2007, 104, 1572.
7. Wooden, D. C.; Lamont, J. C.; Gorka, R. Soc Plast Eng Annu Tech Conf 1986, 44, 675.
8. Todd, W. G.; Enos, C.; Predicting HDPE Melt Index from Gel Permeation Chromatography Data, Int GPC Symp 2000, Las Vegas, NV.
9. Ariawan, A. B.; Hatzikiriakos, S. G.; Goyal, S. K.; Hay, H. Adv Polym Tech 2001, 20, 1.
10. Hinchliffe, M.; Montague, G.; Willis, M.; Burke, A. AIChE J 2003, 49, 2609.
11. Nele, M.; Latado, A.; Pinto, J. C. Macromol Mater Eng 2006, 291, 272.
12. Des Cloizeaux, J. Macromolecules 1990, 23, 4678.
13. Tsenoglou, C. ACS Polym Prep 1987, 28, 185.
14. Tsenoglou, C. Macromolecules 1991, 24, 1762.
15. Des Cloizeaux, J. J. Europhys Lett 1988, 5, 437.
16. Nelder, J. A.; Mead, R. Computer J 1965, 7, 308.
17. Lagarias, J. C.; Reeds, J. A.; Wright, M. H.; Wright, P. E. SIAM J Optim 1998, 9, 112.
18. Himmelblau, D. M. Process Analysis by Statistical Methods; Wiley: New York, 1970.